PCCP

RSC Publishing

PAPER

View Article Online
View Journal

A combined experimental and computational study on the adsorption and reactions of NO on rutile TiO_2†

Cite this: DOI: 10.1039/c2cp42653f

Dorothee Stodt,*[a] Heshmat Noei,*[b] Christof Hättig[a] and Yuemin Wang[b]

Received 31st July 2012,
Accepted 24th October 2012

DOI: 10.1039/c2cp42653f

www.rsc.org/pccp

In this work we combined computational density functional theory with experimental infrared spectroscopy to determine the adsorbate structure of NO and its reaction products N_2O_2, N_2O, and NO_2 on rutile TiO_2. These reactions are important for the photo-catalytic reduction of NO in exhaust gas, but yet little is known about the mechanisms or the intermediates involved. The combination of high-quality ultrahigh vacuum FTIRS data with large scale embedded cluster calculations using an accurate hybrid density functional rendered it possible to identify and assign unambiguously vibrational frequencies for nine species which are formed upon adsorption and reaction of NO on rutile TiO_2. Some of them have been observed for the first time. As a result of the quantum chemical calculations we can report for all adsorbates accurate structures and binding energies.

Published on 25 October 2012 on http://pubs.rsc.org | doi:10.1039/C2CP42653F
Downloaded by Ruhr Universitat Bochum on 23 November 2012

1 Introduction

Besides numerous other applications in which titanium dioxide (TiO_2) has been used since many years, in recent years it has attracted increasing interest as a photo-catalyst for redox reactions, in particular for the oxidation of organic molecules. The main motivation for this interest is that TiO_2 is a cheap and nonhazardous material. It plays also an important role in removing air pollution, because of its ability to act as a photo-catalytic reductant. One of the important applications of TiO_2 is the reduction of NO_x,[1,2] which is released when fossil or other nitrogen containing fuels are burned.

In 1992 Boccuzzi *et al.*[3] discovered that TiO_2 powder samples can reduce NO to N_2O in a thermally activated process. Shortly thereafter Lu *et al.*[4] found that the same reaction takes place on defective TiO_2(110) surfaces. Later, Sorescu *et al.*[5] investigated the adsorption of NO and the formation of N_2O on the oxidized TiO_2(110) surface by temperature-programmed desorption, Auger electron spectroscopy, and low energy diffraction measurements. The experimental study was complemented with periodic plane wave density functional theory (DFT) calculations with pseudo-potentials. As functional a spin-polarized gradient-corrected form of the exchange correlation functional (GGA) was used. Due to the lack of accurate vibrational frequencies an assignment of the experimentally observed species to the possible structures proposed from the results of the DFT calculations was, however, not possible. Some of the authors[6] recently used ultra-high vacuum Fourier transform infrared spectroscopy (UHV-FTIRS) to investigate the adsorption and reduction of NO on a rutile (110) single crystal surface. In general, the intensity of the IR bands of adsorbates on oxide single crystals is only very weak due to the optical properties of dielectric materials, which makes the observation of adsorbate-related IR bands on oxide single-crystal surfaces very difficult. Recently, we have designed a novel UHV-FTIRS apparatus, which creates the possibility to record high-quality IR data for oxide single crystal surfaces. For the NO–TiO_2(110) system, however, the intensity of some IR bands is still too low to be clearly resolved from the background. In the present work we extend the UHV-FTIRS investigations to rutile nanoparticles in order to overcome the problem of low intensities. We performed here IR experiments of NO adsorption on rutile TiO_2 powder samples using the UHV-FTIR spectroscopy. The clean, adsorbate-free TiO_2 powder samples were prepared in the UHV chamber and high-quality and reliable IR bands were obtained after NO adsorption. The corresponding IR spectra show a large number of vibrational bands originating mainly from the formation of various species on the TiO_2(110) surface. This conclusion is supported by the fact that polycrystalline rutile TiO_2 nanoparticles are dominated by the (110) facet.

In this work we combine the high-quality vibrational spectra with *ab initio* periodically embedded cluster calculations for several supposed structures. In particular we determined possible

[a] Lehrstuhl für Theoretische Chemie, Ruhr-Universität Bochum, 44801 Bochum, Germany. E-mail: dorothee.stodt@rub.de; Fax: +49 (0)234 3214045; Tel: +49 (0)234 3224523

[b] Lehrstuhl für Technische Chemie, Ruhr-Universität Bochum, 44801 Bochum, Germany. E-mail: heshmat.noei@rub.de; Fax: +49 (0)234 3214115; Tel: +49 (0)234 3222341

† Electronic supplementary information (ESI) available. See DOI: 10.1039/c2cp42653f

Published on 25 October 2012 on http://pubs.rsc.org | doi:10.1039/C2CP42653F
Downloaded by Ruhr Universitat Bochum on 23 November 2012

adsorption structures for NO, N_2O_2, N_2O and NO_2 and calculated their vibrational signatures. The computed structures and vibrational frequencies are compared with the data from the UHV-FTIR study. The consistent experimental and theoretical results made it possible to assign the bands observed in the UHV-FTIR spectra to detailed adsorbate structures and to provide deeper insight into the microscopic reaction mechanism involving the disproportionation of NO to N_2O and NO_2.

2 Computational method

All calculations in present work have been done with the TURBOMOLE program package[7] at the DFT level using the dscf[8] program. We employed throughout the B3LYP hybrid functional[9–13] which includes in addition to a GGA exchange and correlation functional an Hartree–Fock-like exact exchange to minimize the self-interaction error. In the geometry optimizations the structures were converged to 10^{-3} au. All TZVPP energies were converged up to 10^{-6} au. The grid m3[14] was used. For these calculations we used the periodic electrostatic embedded cluster method[15,16] (PEECM) where the fully quantum mechanically described subsystem is embedded in a periodic point charge array to account for the long ranging Madelung field of the ionic crystal. Compared to three-dimensional periodic plane wave calculations, embedded cluster calculations do not require the pseudo-potential approximation for the atoms in the quantum system and are substantially more efficient in the limit of low coverage and if, as in the current study, hybrid functionals are employed. To prevent at the interface between the quantum system and the point charge array artifacts due to an unphysical strong attraction of electrons by bare positive point charges, the clusters are surrounded by a layer of effective core potentials (ECPs).

All calculations have been done for a cut-out of the (110) surface, which is the most stable surface of rutile[18] and the most abundant one in powder samples. Also from experiment it is known that in IR spectra the intensities of species from other rutile surfaces are very low. To model the (110) surface we used a $Ti_{40}O_{80}$ cluster (cmp. Fig. 1) and a setup for the embedding which in previous studies[19,20] has shown to give essentially converged results in good agreement with the experimental data. The relaxed surface structure was taken from a periodic DFT slab calculation by Kowalski *et al.*[17] As ionic charges for the electrostatic embedding we used the values +3.0 (Ti) and −1.5 (O) which were optimized in ref. 20 on large cluster models. The 217 positive point charges closest to the quantum clusters were augmented with a Ca^{2+}ECP taken from ref. 21 to account for the Pauli repulsion of the titanium ionic cores. In the geometry optimizations the position of the point charges and ECPs and the 30 outermost atoms of the quantum cluster have been held fixed while the positions of all other atoms including the N_xO_y adsorbates are fully optimized. For the N_2O_2 species, which have a small gap between the lowest singlet and triplet states we carried out calculation for both, singlet and triplet, spin states. For the NO and N_2O species only, respectively, doublet and closed-shell singlet states are relevant, if nothing else is mentioned in the result section.

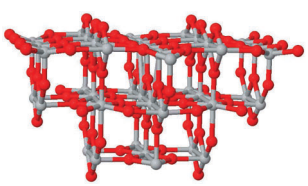


Fig. 1 Model for the (110) rutile surface: $Ti_{40}O_{80}$ cluster for the computational investigations. Its geometry is based on the results of Kowalski *et al.*,[17] while the inner atoms were re-optimized at the B3LYP/DFT level.

Table 1 Scaling factors used for the vibrational frequencies. The factors have been determined as ratios between experimental gas phase fundamental frequencies from ref. 22–25 and the gas phase harmonic values calculated at the B3LYP/SVP level

Structure	Mode	Factor
NO	$\nu_{N-O,str}$	0.92
cis-O–NN–O	$\nu_{N-O,sym}$	0.92
cis-O–NN–O	$\nu_{N-O,as}$	0.98
trans-O–NN–O	$\nu_{N-O,sym}$	0.95
trans-ONN–O	$\nu_{N-O,as}$	0.96
N_2O	ν_{N-N}	0.92
N_2O	ν_{N-O}	0.93
NO_2	$\nu_{N-O,as}$	0.89
NO_2	$\nu_{N-O,sym}$	0.91

For all equilibrium structures we calculated the harmonic vibrational frequencies to simulate the IR spectrum and to compute the zero point vibrational contribution to the adsorption energies. The geometry optimizations and frequency calculations were carried out with the polarized split valence basis set SVP.[26] For comparison with the experimental spectra the computed vibrational frequencies were scaled with the factors shown in Table 1 to correct for the neglect of an harmonicities and systematic errors of the DFT functional and the basis set.

To obtain accurate adsorption energies we have done B3LYP single point calculation with the doubly polarized valence triple-ζ basis TZVPP.[27,28] All reported adsorption energies include the zero point vibrational energy calculated from the unscaled B3LYP/SVP harmonic frequencies.

3 Experimental section

For the UHV-FTIRS measurements the polycrystalline rutile TiO_2 powder samples (Sachtleben, 100 m^2 g^{-1}) were first pressed onto a gold-plated stainless-steel grid (0.5 × 0.5 cm) and then mounted on a sample holder to record FTIR data in transmission mode. It was found crucial to conduct also the powder experiments under UHV conditions. Therefore, UHV-FTIR measurements on rutile TiO_2 powder samples are done with a newly designed UHV apparatus, which combines a state-of-the-art vacuum IR spectrometer (Bruker, VERTEX 80 v) with an UHV system (Prevac).[29] The sample holders, on which the TiO_2 powder samples are mounted after they have been pressed on a grid, are specially designed for the FTIR transmission measurements under UHV conditions. This method allows a

This journal is © the Owner Societies 2012

Published on 25 October 2012 on http://pubs.rsc.org | doi:10.1039/C2CP42653F
Downloaded by Ruhr Universitat Bochum on 23 November 2012

rapid heating and cooling of the samples between 100 and 1000 K.[29,30] The base pressure in the measurement chamber was 2×10^{-10} mbar. To achieve a high sensitivity and stability of the measurements, the adsorption of atmospheric moisture is prevented by evacuating the optical path inside the IR spectrometer and the space between the spectrometer and the UHV chamber. By heating to 750 K, the grid and the attached powder particles were cleaned in the UHV chamber in order to remove all contamination, such as water and hydroxyl groups. Prior to each exposure to NO, a spectrum of the clean TiO_2 powder was recorded as a background reference. All UHV-FTIR spectra were collected with 1024 scans at a resolution of 2 cm^{-1} in the transmission mode. Exposure of the sample to NO was carried out by back-filling the measurement chamber through a leak valve.

4 Results and discussion

4.1 UHV-FTIRS results

Fig. 2 shows the IR spectra recorded for NO adsorption on the pure, adsorbate-free rutile TiO_2 powder sample at 110 K. After NO exposure, a number of IR bands are observed at 1903, 1873, 1752, 1732, 2240 and 1298 cm^{-1}. At higher NO dosage five other bands emerge at 1922, 1705, 1598, 2258 and 1254 cm^{-1}. Recently,[6] it was found that exposing the TiO_2(110) single-crystal surface to NO at 110 K leads to the appearance of three IR bands at 1875, 1750 and 2243 cm^{-1}, which are characteristic of the presence of three surface species, NO, $(NO)_2$ and N_2O, respectively. These bands were observed on both fully oxidized and reduced TiO_2(110) surfaces. The only difference is that the negative bands at 1875 and 1750 cm^{-1} observed for oxidized samples became positive for reduced TiO_2(110), whereas the N_2O band at 2243 cm^{-1} remains negative. This is explained by the different roles of s- and p-polarized light at semiconductor (and insulator) surfaces. Bridging oxygen vacancies act as electron donors yielding an n-type TiO_2 semiconductor.[18] (For further details we refer to ref. 6.) Based on the IR results obtained on a single-crystal TiO_2(110) surface,[6] the intense band at 1873 cm^{-1} is attributed to the N–O stretching mode of an NO monomer adsorbed *via* the N atom on the five-fold coordinated Ti^{4+}sites (Ti_{5c}). The dominating band at 1755 cm^{-1} is assigned to the asymmetric stretching vibration of *cis*-(ONNO) dimers.[6] The corresponding symmetric stretching frequency is the same as that for the adsorbed monomer at 1873 cm^{-1}. The other intense IR band at 2240 cm^{-1} is attributed to the N–N stretching mode characteristic of N_2O adsorbed on Ti_{5c} sites.

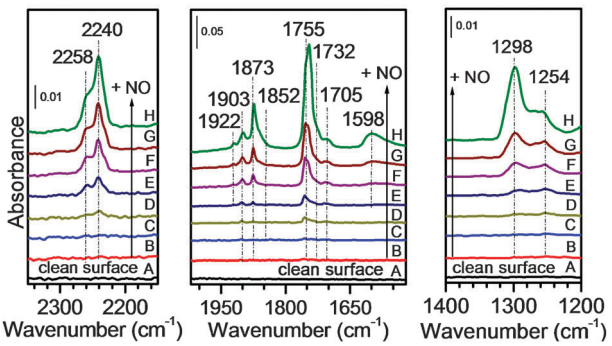


Fig. 2 UHV-FTIR spectra obtained after exposing the clean rutile TiO_2 powder to different doses of NO at 110 K in an UHV chamber. The sample was prepared *via* heating in the UHV chamber to 700 K in order to remove all adsorbed species; (A) clean surface and (B–H) exposure to NO: (B) 1×10^{-7} mbar, (C) 5×10^{-7} mbar, (D) 1×10^{-6} mbar, (E) 5×10^{-6} mbar, (F) 1×10^{-5} mbar, (G) 5×10^{-5} mbar, (H) 1×10^{-4} mbar.

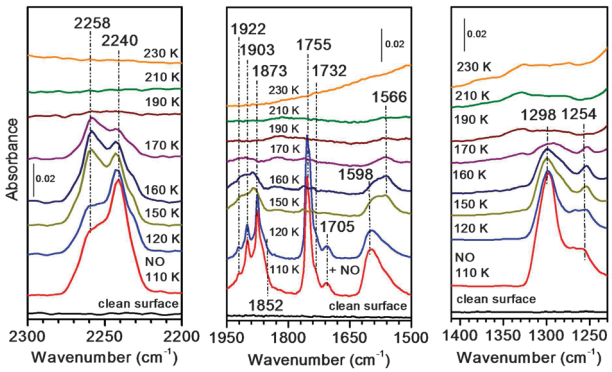


Fig. 3 UHV-FTIR spectra obtained after exposing the clean rutile TiO_2 powder to NO (1×10^{-4} mbar) at 110 K in an UHV chamber and subsequent heating to the indicated temperatures.

In order to get more information about the thermal stability of different species on rutile TiO_2 powder surfaces, the sample was heated to higher temperatures after exposure to NO at 110 K. The temperature-dependent IR spectra (Fig. 3) show that no new vibrational bands are observed with heating to higher temperatures. The IR bands in the frequency range of 1950–1700 cm^{-1} decrease quickly in intensity and disappear completely at about 170 K, revealing that the NO monomer and dimer species are weakly bound to rutile TiO_2 surfaces. The dominating IR bands at 2258, 2240, and 1254 cm^{-1}, which are characteristic of the formation of N_2O *via* NO reduction, are removed totally upon annealing to 190 K. Finally, the intense IR bands at 1598, 1566 and 1298 cm^{-1} disappear also at about 190 K. They indicate the presence of NO_2 species formed *via* NO oxidation, as discussed in detail below.

4.2 Computational results

For all four investigated molecules (NO, N_2O_2, N_2O, NO_2) we found on the TiO_2(110) surface only adsorption sites where these species are bound to a fivefold coordinated titanium cation (Ti_{5c}). For the adsorption of a single nitrogen oxide on the cluster surface we found in agreement with ref. 5 two equilibrium structures shown in Fig. 4: NO can bind either with oxygen (O_{ad}) or with nitrogen (N_{ad}) to the surface. The bond distances are 2.49 and 2.47 Å for the Ti–O bond in NO (O_{ad}) and the Ti–N bond in NO (N_{ad}), respectively. For both structures the angle between the N–O bond and the bond to the fivefold coordinated titanium atom is $\approx 130^\circ$.

The N–O stretch frequency of 1893 cm^{-1} is for NO (N_{ad}) nearly the same as in the gas phase (1876 cm^{-1}), whereas NO (O_{ad}) possesses a significantly lower N–O vibration at 1755 cm^{-1}

Published on 25 October 2012 on http://pubs.rsc.org | doi:10.1039/C2CP42653F
Downloaded by Ruhr Universitat Bochum on 23 November 2012

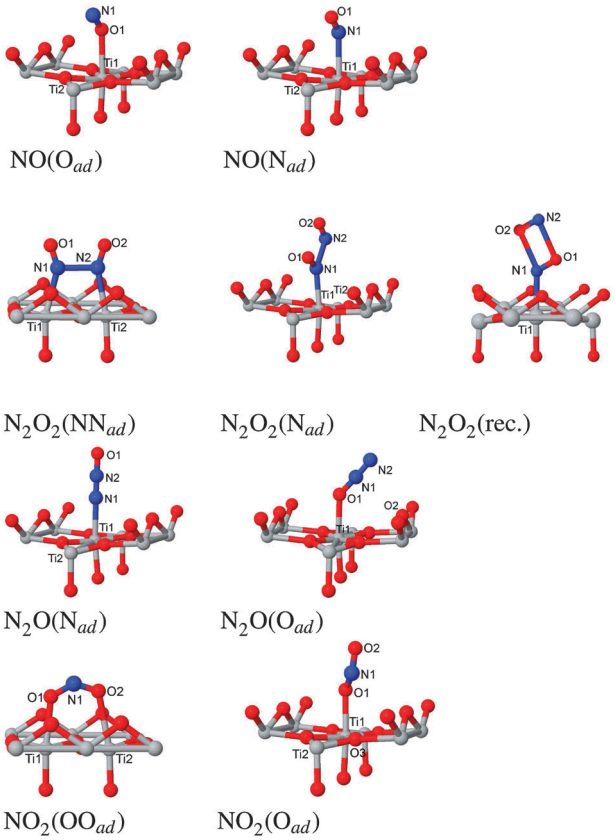


Fig. 4 Equilibrium structures found with DFT/B3LYP for different N_xO_y species adsorbed on the rutile (110) surface.

Table 2 Adsorption energies (E_{ad} in kJ mol^{-1}) and characteristic vibrational frequencies (in cm^{-1}) and intensities (in km mol^{-1}) for different N_xO_y species on the TiO_2(110) surface. For the technical details of the DFT calculation see text, experimental frequencies have been obtained by UHV-FTIR spectroscopy on TiO_2 powder. The adsorption energies of the N_2O_2 species are reported relative to two isolated NO monomers in the gas phase as a reference point. In gas phase the experimental dimerization energy of NO is 10.5 kJ mol^{-1} (ref. 31)

Structure	E_{ad}	Mode	ν_{exp}	ν_{calc}	$I_{\nu_{calc}}$
NO (N_{ad})	−34.6	ν_{NO}	1873	1893	454
NO (O_{ad})	−13.6	ν_{NO}	1732	1755	838
N_2O_2 (NN_{ad})	−62.7	$\nu_{s,O-NN-O}$	1903	1877	557
		$\nu_{a,O-NN-O}$	1752	1763	290
N_2O_2 (N_{ad})	−77.7	$\nu_{s,O-NN-O}$	1922	1951	1554
		$\nu_{a,O-NN-O}$	1852	1823	128
N_2O_2 (rec.)	−59.3	ν_{N-O2}	—	2051	1692
		ν_{N-O1}	—	1759	104
N_2O (N_{ad})	−32.8	ν_{N-N}	2258	2289	983
		ν_{NN-O}	—	1366	11
N_2O (O_{ad})	−29.8	ν_{N-N}	2240	2250	283
		ν_{NNO}	1254	1227	199
NO_2 (O_{ad})	−39.1	ν_{N-O2}	1598	1629	418
		ν_{N-O1}	1254	1249	159
NO_2 (OO_{ad})	−32.2	$\nu_{a,O-N-O}$	1566	1611	204
		$\nu_{s,O-N-O}$	1298	1310	5

(cmp. Table 2). According to the calculated adsorption energies listed in Table 2 the coordination with the nitrogen atom to the Ti_{5c} center is more favorable (by about 11 kJ mol^{-1}) than the coordination with the O atom. At first glance it seems counter-intuitive that the shift of the vibrational frequency (relative to the gas phase value) is much smaller for the more stronger bound N_{ad} species. The reason for this phenomenon is the mixed π*-dz and 5σ-dz character of the NO–Ti bond. The coordination of the halfoccupied π* orbital causes a blue shift of ν_{N-O}, while the coordination of the 5σ orbital to Ti_{5c} causes a red shift. The overall shift of ν_{N-O} depends on the balance between these two contributions. In NO π* is polarized to the N atom and thus the π*–dz bond in NO (N_{ad}) is stronger than in NO (O_{ad}). As a consequence the significant red shift of ν_{N-O} observed for NO (O_{ad}) is in NO (N_{ad}) compensated by the blue shift from the π*–dz condition. The experimental result obtained by first-order desorption kinetic analysis for an adsorption energy of −35.2 kJ mol^{-1} (ref. 5) agrees very well with the present DFT value for NO (N_{ad}); the difference is less than 1 kJ mol^{-1}. Xu *et al.*[6] reported for this species an experimental NO stretch frequency of 1875 cm^{-1}. The UHV-FTIR spectra show a band at 1873 cm^{-1}, which is in agreement with both the experimental and the computed vibrational frequency. Also for NO (O_{ad}) the agreement between the current experimental (1732 cm^{-1}) and computed (1755 cm^{-1}) NO stretch frequencies is good and substantiates the presence of NO (O_{ad}) as minority of NO monomer species on the rutile TiO_2 surface. Sorescu *et al.*[5] investigated different possible adsorption structures for NO on TiO_2 and found the NO (N_{ad}) species to be most stable. For half coverage of the TiO_2(110) surface they found besides a structure, in which the NO molecules are—similar to those in Fig. 4—oriented perpendicular to the ($\bar{1}$10) plane a second minimum with the NO molecules positioned in the ($\bar{1}$10) plane, which is ≈0.1 kJ mol^{-1} lower in energy. We only find an equilibrium structure with NO perpendicular to the ($\bar{1}$10) plane. This is related to the fact that the current calculations are done for the low coverage limit. Later, Rodriguez *et al.*[32] computed the adsorption energy of NO *via* nitrogen on rutile (110) to test the setup for a computational study of the oxidation of NO_2 on rutile. However, the binding energy of −48.3 kJ mol^{-1} which they obtained is 40% higher than our present result and about 13 kJ mol^{-1} above the experimental value of ref. 5.

We also explored the formation of a $(NO)_2$ dimer and were able to identify three possible structures (Fig. 4). Two of them are *cis*-(ONNO) species: N_2O_2 (NN_{ad}) and N_2O_2 (N_{ad}). The third species, N_2O_2 (rec.), has a rectangular structure with two short and two long N–O bonds. N_2O_2 (NN_{ad}) is bidentate bonded to two Ti_{5c} centers and composed of two weakly coordinated NO monomers adsorbed next to each other, while N_2O_2 (N_{ad}) is a $(NO)_2$ dimer bonded monodentate to a single Ti_{5c} center. In the bidentate structure both nitrogen atoms have the same distance to the neighboring titanium atoms (2.41 Å) and also the two O–N–N angles are the same (107°). In contrast to this both monodentate N_2O_2 structures have a shorter N–Ti bond distance of about 2.3 Å.

The adsorption energies of the bidentate (−62.7 kJ mol^{-1}) and rectangular (−59.3 kJ mol^{-1}) structures differ only by about 3 kJ mol^{-1}, while the monodentate *cis* structure is with −77.7 kJ mol^{-1} about 20 kJ mol^{-1} more favorable. Its symmetric and anti-symmetric O–NN–O vibrational stretch frequencies are

This journal is © the Owner Societies 2012

Published on 25 October 2012 on http://pubs.rsc.org | doi:10.1039/C2CP42653F
Downloaded by Ruhr Universitat Bochum on 23 November 2012

determined to be 1951 and 1823 cm^{-1}, respectively. It should be noted that it will be hard to resolve the anti-symmetric mode in experimental IR spectra since its intensity is about an order of magnitude weaker than that of the symmetric mode. The DFT result for the symmetric mode, however, agrees well with the value from the UHV-FTIR measurement of 1922 cm^{-1} demonstrating the formation of monodentate N_2O_2 species on rutile TiO_2 powder samples.

For the bidentate N_2O_2 species the current DFT calculations predict the symmetric O–NN–O stretch frequency at 1877 cm^{-1}, which is close to the frequency for the NO stretch mode in the N-bound NO species on TiO_2. This has recently also been observed by Xu *et al.*[6] The corresponding antisymmetric mode is predicted by the DFT calculations at 1763 cm^{-1}, which is in good agreement with the result on TiO_2(110) and also with the current experimental UHV-FTIR result of 1752 cm^{-1} on TiO_2 powder samples. The rectangular N_2O_2 (rec.) species have compared to the *cis* structures only weakly coupled O–NN–O vibrational stretching frequencies (2051 cm^{-1}, 1759 cm^{-1}) and the intensity of the anti-symmetric stretching frequency (1759 cm^{-1}) is again very low (only about 6 percent of the other). We found, however, no experimental evidence for the formation of this species.

For all three N_2O_2 structures the adsorption geometries and energies were also computed by Sorescu *et al.*,[5] who also found the singlet states to be more stable than the triplets. They obtained, however, a different energetic order for three species. The DFT/GGA slab calculations predicted N_2O_2 (NN_{ad}) with −57.3 kJ mol^{-1} to be the most stable species followed by N_2O_2 (rec.) (−48.4 kJ mol^{-1}). N_2O_2 (N_{ad}) was predicted to be the least stable species with an adsorption energy of −44.2 kJ mol^{-1} which is almost 26 kJ mol^{-1} higher than the current DFT/B3LYP result. It is, however, not clear whether the origin of this discrepancy is the different density functional and computational setup or the fact that calculations in ref. 5 have been carried out for full coverage, where repulsive lateral interaction might reduce the binding energy. The difference in the adsorption geometries obtained in the current calculations and those of ref. 5 is mostly in the range of a few pm. One exception is the N–N distance in N_2O_2 (NN_{ad}). While the present calculations predict it to be 2.41 Å, Sorescu *et al.* obtained a 50 pm shorter bond distance.

We also investigated three additional N_2O_2 species proposed in ref. 5, which are shown in Fig. 5. In the structures TS1 and TS2 all N–O distances are 1.34 ± 0.01 Å and the angles between the atoms in both quadrilaterals are about 90°. TS1 is, compared to TS2, rotated by 70° around the N–Ti axis and tilted by about 8° towards the bridging oxygens. TS3 has an N–N bond and both oxygens are bonded to the same N atom. The N–Ti distances are for all three species relatively short compared to species in Fig. 4: 2.26 Å and 2.32 Å for TS1 and TS2, respectively, and 2.26 Å for TS3. All three transition states decomposed to N_2O_2 (rec.), if allowed to relax. Of all investigated structures, TS3 is the only one, for which the triplet state is more stable than the singlet.

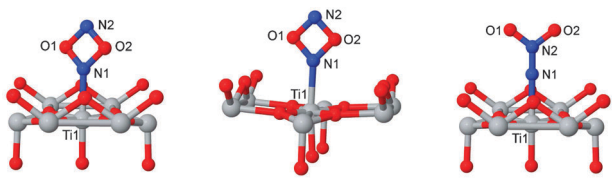


Fig. 5 With DFT/B3LYP optimized structures for transition states (left: TS1; center: TS2; right: TS3).

For the reduced nitrogen oxide, N_2O, two stable structures were found in the DFT calculations (cmp. Fig. 4): one structure, in which the terminal nitrogen atom binds to a Ti_{5c}, N_2O (N_{ad}), and one structure where the oxygen binds to the surface, N_2O (O_{ad}). The N_2O (N_{ad}) species adsorbs in a linear geometry almost perpendicular to the surface with a N–Ti bond distance of 2.27 Å and a N–N–O angle of 179°. The N–N stretch frequency of N_2O (N_{ad}) is predicted by the DFT/B3LYP calculations at 2289 cm^{-1}. The next lower frequency is that of the (NN)–O stretch mode at 1366 cm^{-1}. Compared to the gas phase both frequencies are blue shifted. In N_2O (O_{ad}) the adsorbate is orientated almost perpendicular to the Ti_{5c} rows and its Ti–O bond distance is 2.27 Å. For this species the N–N stretch frequency is with 2250 cm^{-1} slightly lower than in N_2O (N_{ad}) but still blue shifted compared to the gas phase. The (NN)–O stretching frequency is with 1227 cm^{-1} about 100 cm^{-1} lower than in N_2O (N_{ad}). However, its intensity is only about 1% of that of the N–N stretch mode. With adsorption energies of −32.8 kJ mol^{-1} and −29.8 kJ mol^{-1} the two structures are similar in energy.

Some of us determined the N–N stretching frequency with UHV-FTIR spectroscopy on single crystal TiO_2(110) surfaces for N_2O.[6] Its value of 2243 cm^{-1} agrees well with current DFT result for the N_2O (O_{ad}) adsorption structure. Rusu and Yates[33,34] detected in their study on the adsorption of N_2O on TiO_2 both N- and O-bound species, which are identified by two main band pairs at 2262 and 1313 cm^{-1} and at 2237 and 1251 cm^{-1}. In the present UHV-FTIRS results (cmp. Table 2), we found that after NO adsorption on TiO_2 powders at 110 K two dominating IR bands appear at 2258 and 2240 cm^{-1} in excellent agreement with the results obtained from N_2O adsorption by Rusu and Yates.[33,34] They are characteristic of the presence of N- and O-bound N_2O species formed *via* NO reduction at perfect Ti^{4+} sites, as further confirmed by the current DFT/B3LYP calculations. In addition, the intense IR band at 1254 cm^{-1} is assigned to the ν(NN–O) stretch mode of the O-bound N_2O species. The fact that for the N-bound N_2O species the intensity of the N–O stretch mode is too weak to be measurable fits to results of the DFT calculations. It should be noticed that in addition to the two major N_2O species formed on perfect Ti^{4+} sites, Rusu *et al.* detected two very weak band pairs at 2245 and 1234 cm^{-1} and 2297 and 1324 cm^{-1}, which could be related to the N_2O species adsorbed at sites close to defects. In our IR spectra the N_2O related IR bands show clearly a broadening revealing the presence of other minor N_2O species due to the complexities of TiO_2 powder particles.

Sorescu *et al.*[5] obtained in their DFT/GGA calculations for the N_2O (N_{ad}) and N_2O (O_{ad}) species on the defect free surface the same energetic order as in the current DFT/B3LYP calculations.

Published on 25 October 2012 on http://pubs.rsc.org | doi:10.1039/C2CP42653F
Downloaded by Ruhr Universitat Bochum on 23 November 2012

They found, however, at 50% coverage a larger splitting of 15 kJ mol^{-1} between the adsorption energies for the two species. While the GGA result for N_2O (N_{ad}) was about the same as the current B3LYP value, the GGA result for the binding energy of the O-bound species was 12 kJ mol^{-1} smaller. This is probably related to somewhat different adsorption geometries of the O-bound N_2O structure: while we obtained in the B3LYP calculations for the equilibrium structure in the zero coverage limit a slightly tilted geometry, the structure reported in ref. 5 is oriented vertical to the $(\bar{1}10)$ plane. Sorescu *et al.* showed that the binding energies for the N-bound species are again sensitive to the concentration of the adsorbate. With increasing concentration of molecules on the surface the binding energy decreases. At full coverage it is reduced by about 50% to only −15.8 kJ mol^{-1}. Probably related to the difference in coverage is the fact that the bond distances obtained in ref. 5 for N_2O (N_{ad}) and N_2O (O_{ad}) to Ti_{5c} are about 10 and 60 pm longer than the current DFT/B3LYP results.

For NO_2 we found in the B3LYP calculations two structures for the adsorption on the rutile (110) surface, which differ only by about 7 kJ mol^{-1} in energy (Fig. 4). One bidentate structure, NO_2 (OO_{ad}), with O–Ti bond distances of 2.39 Å and 2.76 Å and a second structure, NO_2 (O_{ad}), which binds to the (110) surface in a monodentate configuration with d_{Ti-O} = 2.27 Å. The monodentate structure has two almost uncoupled N–O modes with frequencies of 1629 cm^{-1} (ν_{N-O1}) and 1249 cm^{-1} (ν_{N-O2}). For the former, the frequency is close to the gas phase value (1618 cm^{-1}), whereas the other frequency is red-shifted by 40 cm^{-1}. In contrast to the monodentate species, the vibrational frequencies of the bidentate bound NO_2 (OO_{ad}) species are strongly coupled. The values for antisymmetric and symmetric stretching modes are predicted by the DFT/B3LYP calculations at 1611 and 1310 cm^{-1}, respectively. Both values are close to the gas phase frequencies for NO_2. While we found for NO_2 only adsorption structures where the molecule is bound through oxygen atoms to the surface, Sorescu *et al.*[5] reported also one structure which is bound with the nitrogen atom to the surface. This structure could, however, not be reproduced with the current computational setup as equilibrium structure, but converted to one of the O-bound species ($NO_2(O_{ad})$). Also Rodriguez *et al.*[32] investigated the adsorption of NO_2 on the TiO_2(110) surface and found two O-bound species with similar structures as those shown in Fig. 4, even though they obtained with DFT/GGA slab calculations adsorption energies which are about a factor of two larger than the current B3LYP results. The energetic order of the two O-bound NO_2 species, however, agrees with our current results.

4.3 Conclusion

Table 2 shows a complete comparison of the current experimental UHV-FTIRS and computational DFT/B3LYP results for the N–N and N–O stretch frequencies and the computed adsorption energies of the investigated N_xO_y species on the rutile (110) surface. In accord with the DFT calculations, the experimental bands at 1873 and 1732 cm^{-1} are assigned to the N–O stretch modes of two NO monomer species adsorbed, respectively, *via* bonds between the N and the O atom to a fivefold coordinated Ti^{4+} site (Ti_{5c}). The N-bound structure is the major species. It has a considerably higher binding energy than the O-bound species and the experimentally observed adsorption energy[5] of −35.2 kJ mol^{-1} is attributed to the NO (N_{ad}) species. The good agreement between the experimentally observed band at 1732 cm^{-1} with the value of 1755 cm^{-1} predicted by the DFT calculations for the O-bound species shows that NO is also adsorbed in this binding mode.

The assignment of the IR bands at 1903 and 1752 cm^{-1} to, respectively, the symmetric and antisymmetric O–NN–O stretch modes of *cis*-(ONNO) dimers on TiO_2, is clearly confirmed by the computational results. For this species the measured and the computed frequencies agree within a few wavenumbers. In ref. 5 the authors concluded that N_2O_2 dimers are formed spontaneously when two NO molecules adsorb next to each other on the rutile surface. Our observation that the N_2O_2-related IR bands are the dominating ones already at very low coverage supports this conclusion.

The second group of bands at 1922 and 1852 cm^{-1}, which was not observed in the previous measurements on the rutile TiO_2(110) single crystal surfaces,[6] is verified by the DFT/B3LYP calculations to belong to the ν_s and ν_{as} O–NN–O stretch modes of a monodentate *cis*-N_2O_2 species adsorbed through an N–Ti bond. The DFT calculations predicted furthermore a very low intensity for the ν_{as} mode of this species which explains why this mode is only observed as a weak shoulder in the IR spectrum. We could not identify the N–O stretch modes of the cyclic N_2O_2 (rec.) species in the FTIR spectra and conclude that this species is either not at all formed or only in very low concentration.

The DFT/B3LYP calculations verify that the monodentate dimeric $(NO)_2$ (N_{ad}) species has in the limit of low coverage a larger binding energy than N_2O_2 (rec.) and bidentate *cis*-N_2O_2 species. Previous calculations showed that for a coverage of 50% the dimeric $(NO)_2$ (NN_{ad}) is highest in energy.[5] Therefore the energetic order probably changes with increasing coverage. There are two possibilities for the formation of the N_2O_2 (N_{ad}) species during the adsorption of NO: either from a bidentate N_2O_2 species by breaking one N–Ti_{5c} bond or from an NO (N_{ad}) species by the adsorption of a second NO molecule. In any case it is likely an important intermediate for the formation of N_2O.

The DFT/B3LYP calculations give proof to the assumed reduction of NO to N_2O as the computed stretch frequencies of 2250 cm^{-1} (N–N) and 1227 cm^{-1} (NN–O) for the O-bound N_2O species agree well with the bands observed in the UHV-FTIR spectra. Furthermore, an additional band appears at 2258 cm^{-1}, which is characteristic of the formation of N-bound N_2O species and is assigned to the ν_{N-N} mode, where the intensity predicted by the calculations for ν_{NN-O} mode of N-bound N_2O is too low to be detected in the FTIR measurements. We thus conclude that two N_2O species (N- and O-bound) are formed during the reaction of NO with rutile surfaces. A comparison with experimental results by Rusu and Yates,[33,34] where for both species two slightly different adsorption sites were observed, reveals that the bands observed in the

This journal is © the Owner Societies 2012

Published on 25 October 2012 on http://pubs.rsc.org | doi:10.1039/C2CP42653F
Downloaded by Ruhr Universitat Bochum on 23 November 2012

current UHV-FTIR measurements on TiO_2 powder samples correspond predominantly to the formation of N_2O species at perfect Ti^{4+}sites on the (110) surface, as supported by the computational results. The broadness of the N_2O related IR bands matches the presence of other minor N_2O species at defect sites or on other facets of rutile TiO_2 powder particles.

The experimental IR bands at 1566 and 1298 cm^{-1} were primarily assigned based on the frequencies and the thermal stability to vibrations of O–N–O species adsorbed on TiO_2. The DFT/B3LYP calculations confirm this assumption, revealing the formation of a bidentate NO_2 (OO_{ad}) species *via* NO oxidation on TiO_2. In accordance with the theoretical results, the intense band at 1598 cm^{-1} is characteristic of the existence of a monodentate NO_2 (O_{ad}) species. The corresponding ν_{O-N-O} mode could be overlapped with the ν_{NN-O} mode of the N_2O at 1254 cm^{-1}.

We could currently not assign the band observed in the UHV-FTIR spectra at 1705 cm^{-1}. It might be that this band belongs to species at defects or on a different surface. Overall there is a good agreement between the computational and the experimental results, which encourages us to suggest the following mechanism for the disproportionation of NO on TiO_2 surfaces:

$$2NO_{ad} \rightarrow N_2O_{2,ad}$$

$$N_2O_{2,ad} \rightarrow N_2O + O_{ad}$$

$$NO + O_{ad} \rightarrow NO_2$$

After adsorption on the TiO_2 surface NO first dimerizes to N_2O_2 which is decomposed to N_2O and an oxygen atom attached to the TiO_2 surface, probably bound to a defect or at a (step) edge. The oxygen atom can later react with another NO molecule to form NO_2.

Acknowledgements

The work reported here has been supported by the Deutsche Forschungsgemeinschaft (DFG) through the Collaborative Research Center SFB 558 ''Metal–Substrate Interactions in Heterogeneous Catalysis'' and its integrated graduate school.

References

1 T. L. Thompson and J. T. Yates, *Chem. Rev.*, 2006, **106**, 4428.
2 R. Schaub, P. Thostrup, N. Lopez, E. Lægsgaard, I. Stensgaard, J. K. Nørskov and F. Besenbacher, *Phys. Rev. Lett.*, 2001, **87**, 266104.
3 F. Boccuzzi, E. Guglielminotti and A. Chiorino, *Sens. Actuators, B*, 1992, **7**, 645.
4 G. Lu, A. Linsebigler and J. T. Yates Jr., *J. Phys. Chem.*, 1994, **98**, 11733.
5 D. C. Sorescu, C. N. Rusu and J. T. Yates, *J. Phys. Chem. B*, 2000, **104**, 4408.
6 M. Xu, Y. Gao, Y. Wang and C. Wöll, *Phys. Chem. Chem. Phys.*, 2010, **12**, 3649.
7 A development of University of Karlsruhe and Forschungszentrum Karlsruhe GmbH, 1989–2007, Turbomole GmbH, since 2007, available from http://www.turbomole.com, TURBOMOLE V6.3, 2011.
8 M. Häser and R. Ahlrichs, *J. Comput. Chem.*, 1989, **10**, 104.
9 P. A. M. Dirac, *Proc. R. Soc. London, Ser. A*, 1929, **123**, 714.
10 J. C. Slater, *Phys. Rev.*, 1951, **81**, 385.
11 A. D. Becke, *Phys. Rev. A: At., Mol., Opt. Phys.*, 1988, **38**, 3098.
12 C. Lee, W. Yang and R. G. Parr, *Phys. Rev. B: Condens. Matter Mater. Phys.*, 1988, **37**, 785.
13 A. Becke, *J. Chem. Phys.*, 1993, **98**, 5648.
14 O. Treutler and R. Ahlrichs, *J. Chem. Phys.*, 1995, **102**, 346.
15 A. M. Burow, M. Sierka, J. Döbler and J. Sauer, *J. Chem. Phys.*, 2009, **130**, 174710.
16 K. N. Kudin and G. E. Scuseria, *Chem. Phys. Lett.*, 1998, **283**, 61.
17 P. M. Kowalski, B. Meyer and D. Marx, *Phys. Rev. B: Condens. Matter Mater. Phys.*, 2009, **79**, 115410.
18 U. Diebold, *Surf. Sci. Rep.*, 2003, **48**, 53.
19 M. Kunat, F. Träger, D. Silber, H. Qiu, Y. Wang, A. C. van Veen, C. Wöll, P. M. Kowalski, B. Meyer, C. Hättig and D. Marx, *J. Chem. Phys.*, 2009, **130**, 144703.
20 D. Stodt and C. Hättig, *J. Chem. Phys.*, DOI: 10.1063/1.4752478.
21 P. Fuentealba, L. v. Szentpaly, H. Preuss and H. Stoll, *J. Phys. Chem. B*, 1985, **18**, 1287.
22 F. Legay and N. Legay-Sommaire, *J. Chem. Phys.*, 1995, **102**, 7798.
23 L. Andrews and M. Zhou, *J. Chem. Phys.*, 1999, **111**, 6036.
24 L. Krim and N. Lacome, *J. Phys. Chem. A*, 1998, **102**, 2289.
25 K. P. Huber and G. Herzberg, *Constants of Diatomic Molecules*, Van Nostrand-Reinhold, New York, 1979.
26 A. Schäfer, H. Horn and R. Ahlrichs, *J. Chem. Phys.*, 1992, **97**, 2571.
27 A. Schäfer, C. Huber and R. Ahlrichs, *J. Chem. Phys.*, 1994, **100**, 5829.
28 K. Eichkorn, F. Weigend, O. Treutler and R. Ahlrichs, *Theor. Chem. Acc.*, 1997, **97**, 119.
29 H. Noei, H. Qiu, Y. Wang, E. Loffler, C. Wöll and M. Muhler, *Phys. Chem. Chem. Phys.*, 2008, **10**, 7092.
30 Y. Wang, A. Glenz, M. Muhler and C. Wöll, *Rev. Sci. Instrum.*, 2009, **80**, 113108.
31 A. F. Holleman, E. Wiberg and N. Wiberg, *Lehrbuch der Anorganischen Chemie*, Walter de Gruyter, Berlin New York, 1995, vol. 101.
32 J. A. Rodriguez, T. Jirsak, G. Liu, J. Hrbek, J. Dvorak and A. Maiti, *J. Am. Chem. Soc.*, 2001, **123**, 9597.
33 C. N. Rusu and J. T. Yates, *J. Phys. Chem. B*, 2000, **104**, 1729.
34 C. N. Rusu and J. T. Yates, *J. Phys. Chem. B*, 2001, **105**, 2596.